ACS SENSORS

Article

Cite This: ACS Sens. 2019, 4, 2375−2380

pubs.acs.org/acssensors

Development of an Immunosensor Based on the Exothermic Reaction between H_2O and CaO Using a Common Thermometer as Readout

Xiaoming Ma,[†,‡,§] Zhen Wang,[‡] Shan He,[‡] Chaoqun Chen,[§] Fang Luo,[§] Longhua Guo,[§] Bin Qiu,[§] Zhenyu Lin,[*,§] Guonan Chen,[§] and Guolin Hong[*,†]

[†]The Department of Laboratory Medicine, The First Affiliated Hospital of Xiamen University, No. 55 Zhenhai Road, Siming District, Xiamen, Fujian 361005, China

[‡]School of Chemistry and Chemical Engineering, Key Laboratory of Organo-Pharmaceutical Chemistry of Jiangxi Province, Gannan Normal University, Ganzhou 341000, P. R. China

[§]MOE Key Laboratory for Analytical Science of Food Safety and Biology, Fujian Provincial Key Laboratory of Analysis and Detection Technology for Food Safety, College of Chemistry, Fuzhou University, Fuzhou, Fujian 350116, China

Supporting Information

ABSTRACT: Thermometers, one of the most commonly used instruments at home, are normally adapted to measure temperature directly with high accuracy but rarely adopted to act as readout in the biosensors. It is necessary to find some ways to establish a relationship between the concentration of the target and the temperature change. In this study, a common thermometer was used as readout to develop a convenient immunosensor. The designed immunosensor comprises three components, including target recognition area, water flow system, and exothermic reaction bottle. The capture antibody for the target [carcinoembryonic antigen (CEA) was selected as a model target] was preloaded on the bottom of the recognition area. In the presence of CEA, a sandwich-type structure was formed between the capture antibody, CEA, and biotinylated detection antibody. Then, the streptavidin-functionalized platinum nanoparticles were labeled on the detection antibody due to biotin−avidin interaction. The captured platinum nanoparticles can effectively catalyze the decomposition of H_2O_2 into O_2. The continuous production of gas resulted in pressure increment inside the reaction bottle and further pushed the water flow into the exothermic reaction bottle. Finally, the water reacted with calcium oxide to generate a large amount of heat in the exothermic reaction bottle; thereby the temperature inside the bottle was enhanced and recorded by a common thermometer easily. The temperature enhancement has a linear relationship with the CEA concentration in the range of 7.81−500 pg/mL with a detection limit of 0.6 pg/mL. Furthermore, by taking advantage of simplicity, compatibility, stability, and high sensitivity, our temperature-based immunoassay has been applied to detect CEA in human serum samples with satisfactory results.

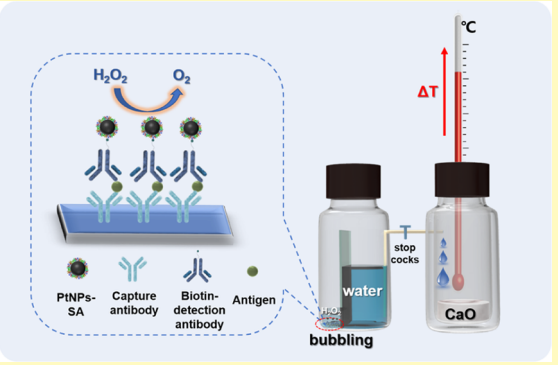

KEYWORDS: *immunosensor, biosensor, cancer diagnosis, carcinoembryonic antigen, temperature, thermometer*

The thermometer is one of the most commonly used devices at home or in the laboratory. However, the applications of mostly commercialized thermometers are still limited in the temperature recording, and little attention had been paid on to act as a signal readout of biosensors. Herein, the key influencing factor is how to transfer the detection signal into temperature changing. To overcome these limitations, many research groups have made some useful attempts.[1,2] For example, Gao's group reported an exothermic chip for quantitative detection of limited heavy metal ions based on the analyte-hydrogel recognition; NaOH powders served as an exothermic reagent, and a forehead thermometer was used to measure the temperature variation.[3] Fu's group introduced a temperature-based measurement strategy based on the nanoparticle-mediated photothermal effect, where a near-infrared (NIR) laser was used to convert the assay signal into heat.[4,5] Alternatively, the liposome-encapsulated indocyanine green was hydrolyzed upon the addition of targets. The released dye converts excitation energy into heat under NIR-laser irradiation, thus allowing the construction of the target-responsive thermometer.[6] These results show that the temperature change in the detection system can be used as an important indicator for the biosensor construction.

Received: May 27, 2019
Accepted: August 7, 2019
Published: August 7, 2019

DOI: 10.1021/acssensors.9b00968
ACS Sens. 2019, 4, 2375−2380

Owing to the antigen−antibody specific recognition system, immunoassay has good selectivity, and it can be applied to detect thousands of targets by simply changing the corresponding antigen−antibody pairs.[7−9] To extend its application in the resource-limited area, the integration of many simple readout techniques (such as barometer, glucose meter, pH meter, naked eyes, etc.) with immunoassay has been developed for the determination of diverse targets.[10−16] However, little attention has been paid to couple with a typical thermometer as readout.

In an early study, we developed a convenient and straightforward aptasensor based on converting molecular recognition into weight variation with an electronic balance as signal readout.[17] The amount of the target enabled us to measure by weighing the discharged water. It is worth noting that self-heating food packaging, which is widely used in the food contents heating without external heat sources can generate a large amount of heat based on the exothermic reaction between calcium oxide (CaO) and water (H_2O).[18] Inspired by this principle, we considered integrating this commonly used exothermic reaction to construct temperature-based immunoassay. Theoretically, 10 μL H_2O reacting completely with CaO powder (2 g) can release 36.51 kJ energy under a closed adiabatic bottle (2.5 mL), which can lead to appropriate 12 °C increment of the air inside the bottle at room temperature. Therefore, a conventional thermometer with high accuracy can record the temperature change of the system.

Herein, we coupled this interesting self-heating reaction with an immunoassay to develop a simple but sensitive immunosorbent-based biosensor. A conventional thermometer was used as the signal readout for the sensitive detection of carcinoembryonic antigen (CEA) (chosen as the model target). The temperature increment was found to be linearly proportional to the concentration of CEA, establishing the quantitative determination of CEA in the human serum samples with satisfactory results.

EXPERIMENTAL SECTION

Preparation of the Capture Antibody Immobilized Glass Vial and Streptavidin-Functionalized Platinum Nanoparticles. The capture antibody immobilization on the glass vial was performed according to the previous report.[19] Besides, the streptavidin (SA)-functionalized platinum nanoparticles (PtNPs) were synthesized based on our previous study.[17] The detail procedures are presented in the Supporting Information.

Design and Fabrication of the Immunosensor Using Thermometer as Readout. The proposed biosensor comprises a target recognition area, water flow system, and exothermic reaction bottle, which separately manufactured and assembled once used (Figure S1). The conventional immunoassay procedure was performed in the target recognition area. After the enzyme catalysis decomposition of H_2O_2 into H_2O and O_2, the pressure inside the bottle (10 mL) dramatically increased. A stopcock was used to control the water flow from the reservoir into the exothermic reaction bottle. Meanwhile, the CaO powder preloaded inside the exothermic reaction bottle (2.5 mL) assembled with a common thermometer reacted with H_2O, and the temperature increment can be recorded by a common thermometer. For the sensitivity determination of CEA, the stopcocks were opened after H_2O_2 decomposition reaction of 15 min. Thus, the suddenly increased pressure pushes the water flow from the target recognition bottle into the exothermic reaction bottle to generated temperature increment.

Analytical Procedure of the Detection. First, 200 μL aliquots of CEA samples in sample dilution buffer (50 mM Tris, 0.14 M NaCl, 1% bovine serum albumin, 0.05% Tween 20, pH 8.0) were added to the capture antibody immobilized glass vial and incubated for 2 h at room temperature. Each glass vial was washed three times with 500 μL wash buffer (50 mM Tris, 0.14 M NaCl, 0.05% Tween 20, pH 8.0), and then, remains of wash buffer was removed via inverting the glass vial and blotting it against clean paper towels after the last wash. The biotinylated detection antibody (100 μL, 1.0 μg/mL) in dilution buffer was added and incubated for 1 h at 37 °C. The washing step was repeated, and then, PtNPs−SA conjugation (100 μL, 0.5 nM) was added with incubation for 30 min at room temperature. After repetition of washing steps, H_2O_2 (1 mL, 30 wt %) was added to the vial and the twist cap was sealed immediately, while the stopcocks were closed at this moment. The bound PtNPs would catalyze the dissociation of H_2O_2 to H_2O and O_2, leading to the increment of pressure inside the bottle. After the catalysis reaction for 15 min, the stopcocks were opened. The generated pressure difference would finally push the water flow into the exothermic reaction bottle. The resulting exothermic reaction of CaO dissolution in the water was monitored by a common thermometer after 5 min of reaction time, and the temperature increment was readout by the naked eye. The sensitivity of this temperature-based sensing platform can be regulated by adjusting the enzymatic reaction time of PtNPs. To meet the requirement of actual sample determination, we control the catalysis reaction time at 5 min.

RESULTS AND DISCUSSION

Principle of Immunosensor Using a Thermometer as Readout. The principle of the proposed immunosensor using a common thermometer as readout is shown in Scheme 1. The

Scheme 1. Principle of the Temperature-Based Immunosensor Using a Common Thermometer as Readout

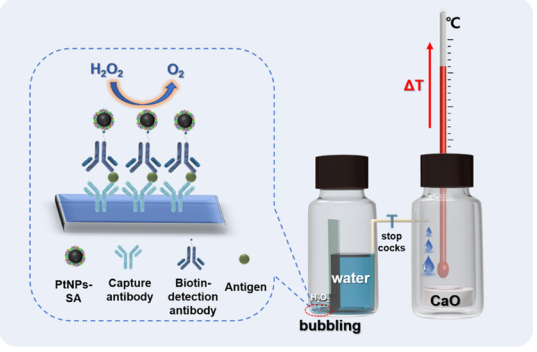

mouse anti-CEA monoclonal antibody (act as the capture antibody) had been preloaded on the bottom of a glass vial first. The biotinylated rabbit anti-CEA polyclonal antibody was used as the detection antibody. Upon the addition of the target (CEA in this study), a sandwich-type structure will form between the capture antibody−CEA-detection antibody. Then, the PtNPs−SA was modified on the sandwich structure through biotin−SA interaction. After repeating washing steps to eliminate the excess unbounded PtNPs−SA, the glass vial was sealed immediately after the addition of H_2O_2. The pressure inside the vial increased gradually as the decomposition of H_2O_2 by PtNPs−SA when the stopcocks were closed. Once the stopcocks were turned on, a certain amount of water would flow into the exothermic reaction bottle immediately due to the pressure difference. The reaction between water (H_2O) and the calcium oxide (CaO, which was preloaded in the exothermic reaction bottle) produces a large amount of heat through the following reaction: CaO (s) + H_2O (l) → $Ca(OH)_2$; $\Delta H = -65.2$ kJ·mol^{-1}. This enormous heat will induce the temperature enhancement of the system

DOI: 10.1021/acssensors.9b00968
ACS Sens. 2019, 4, 2375−2380

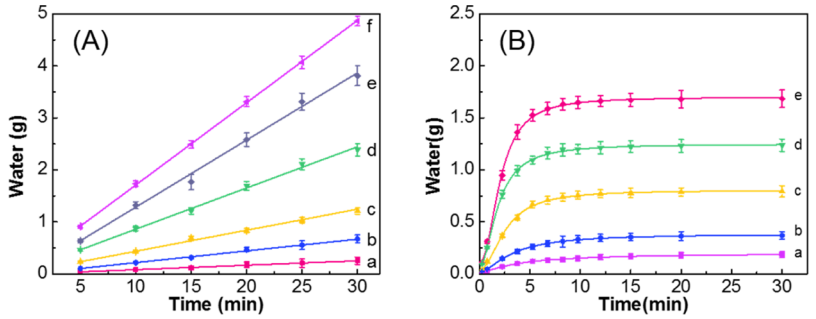

Figure 1. (A) Catalytic decomposition of H_2O_2 with different concentrations of PtNPs−SA in 30 wt % H_2O_2 at different times, the concentration of PtNPs−SA from (a to f) were 10, 25, 50, 100, 150, 200 pM, respectively; (B) catalytic decomposition of H_2O_2 with different concentrations of catalase in 30 wt % H_2O_2, and the concentration of catalase from (a to e) were 2.5, 5, 10, 15, 20 nM, respectively.

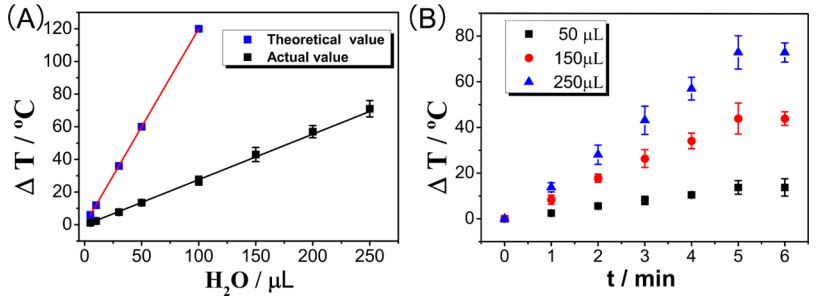

Figure 2. (A) Comparison of the theoretical and actual temperature changing values after the reaction of different amounts of water with the CaO powder (2 g); (B) temperature increment with different amounts of water (50, 150, 250 μL) reacted with the CaO powder (2 g) at different times.

and which can be detected by a common thermometer easily. Thus, the relationship between temperature enhancement and the target concentration can be established successfully. Based on this principle, a simple immunosensor was designed using a simple thermometer as readout.

Characterization of the PtNPs−SA Conjugates. Compared with the catalase enzyme, PtNPs can effectively catalyze the breakdown of H_2O_2 to generate abundant O_2 without apparent deactivation, inducing a significant increase in pressure of the sealed container.[20] To improve the versatility of PtNPs in the application of immunoassay, PtNPs had been conjugated with SA, and the synthetic process was characterized by UV−vis absorption assay. As shown in Figure S2A, the absorbance of H_2PtCl_6 shifts from 259 to 300 nm after the incubation with ascorbic acid, and the color of the solution changes from light yellow to brown, suggesting the successful synthesis of PtNPs. Then, the prepared PtNPs had been conjugated with SA, and the UV−vis absorbance spectra show no significant change. Transmission electron microscopy (TEM) and dynamic light scattering assays are performed to confirm whether the SA had been successfully modified on the PtNPs. The hydrodynamic diameter increases from 72 to 88 nm, and the zeta potential increases from −40.6 to −34.9 mV after the conjugation (Figure S3). These results indicate that the PtNPs−SA conjugates had been well-synthesized. The TEM image of the dendritic nanoparticles (Figure S2B) indicates that the nanoparticles have good dispersion and uniform size with an average diameter ∼25 nm, thus allowing its further modification on the biotin-conjugated antibody.

To study the suitability of PtNPs−SA in the catalytic decomposition of H_2O_2, we compared its catalytic performance with catalase enzyme through the drainage experiment. A certain amount of PtNPs−SA or catalase was added into the 30% H_2O_2 solution to initiate the gas-generation reaction. A large amount of oxygen produced base on the catalysis reaction result in a significant pressure increase, thereby a certain amount of water flowed to the exothermic bottle as a result. The amount of discharged water can be recorded by an electronic balance. As shown in Figure 1A,B, both PtNPs−SA and catalase can push the movement of water flow as a function of time, and this phenomenon is induced solely by the O_2 generated from the decomposition of H_2O_2. However, the catalase enzyme fails to catalyze the O_2 generation after 5 min. Moreover, the catalysis efficiency of catalase would dramatically decrease under high H_2O_2 concentration (data not shown), which can be attributed to the destructive effect of catalase under high concentration of H_2O_2.[21] In comparison to nature catalase, the PtNPs−SA shows increased catalytic ability with increasing H_2O_2 concentration and remains with steady catalytic activity over a long period of time. The catalysis process of PtNPs−SA toward H_2O_2 is a zero-order reaction, so the amount of the discharged water increased almost linearly with the extension of the reaction time.[19] Furthermore, the amount of water has a direct linear relationship with the concentration of PtNPs−SA (Figure S4). Therefore, we can meet the specific requirement of sensitivity by adjusting the reaction time and PtNPs−SA amount.

Measurement of an Exothermic Reaction. A small amount of water reacting completely with CaO powder (2.0 g) can lead to a huge temperature increment in a closed adiabatic bottle (2.5 mL) theoretically. However, the actual temperature increment measured by our method is much lower than that of the theoretical calculation (shown in Figure 2A). The main reason lies in that the external thermal absorption from the reaction bottle and reagents (such as CaO, $Ca(OH)_2$, and etc.). As shown in Figure 2B, the temperature increases gradually as a function of reaction time after mixing CaO with H_2O and finally reach the maximum value at 300 s (5 min).

DOI: 10.1021/acssensors.9b00968
ACS Sens. 2019, 4, 2375−2380

Moreover, the temperature increment enhances with the increasing amount of water added. Therefore, it is possible to utilize these phenomena for further study.

Performance of the Temperature-Based Immunosensor. The variation of temperature responses recorded by a common thermometer with different concentrations of CEA (the stop cock requires to be opened after 15 min of H_2O_2 decomposition reaction) is shown in Figure 3A. The degree of

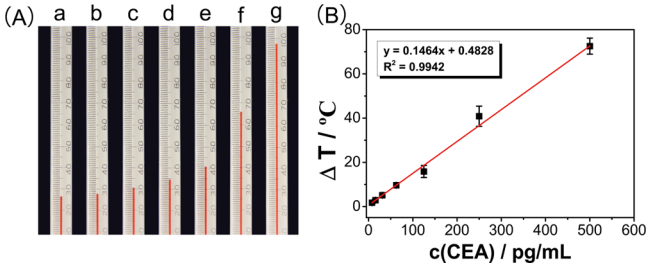

Figure 3. (A) Optical images of temperature increment recorded by the thermometer. The concentrations of CEA from left to right were 7.81, 15.6, 31.2, 62.5, 125, 250, and 500 pg/mL, respectively; (B) plot of the temperature increase (ΔT) vs the concentration of CEA in the sample.

temperature increment has a linear relationship with CEA concentration in the range from 7.81 to 500 pg/mL (Figure 3B) with a correlation coefficient of 0.994. The regression can be expressed as follows

$$\Delta T = 0.1464C(\mathrm{CEA}) + 0.4828$$

where the temperature increase (ΔT) is defined as the temperature change of the bottle before and after the exothermic reaction, and C(CEA) is the concentration of CEA. The limit of detection is 0.6 pg/mL (defined as three standard deviations above the mean background signal), which is more sensitive compared to that of some previous reports (Table S1).[22−28] Thus, the proposed sensing platform can sufficiently satisfy the need for practical applications in the areas of daily life.

To evaluate the specificity of the proposed biosensor for CEA detection, some common proteins present in the serum was selected as negative controls, including human serum albumin (HSA), immunoglobulin G (IgG), prostate-specific antigen (PSA), and hepatitis B surface antigen (HBsAg). As shown in Figure 4, a significant temperature increment is recorded in the presence of CEA (150 pg/mL), but nearly no temperature change is observed even when the concentration of interferents (1500 pg/mL) was ten times than that of CEA. Therefore, these outcomes indicate that our proposed strategy

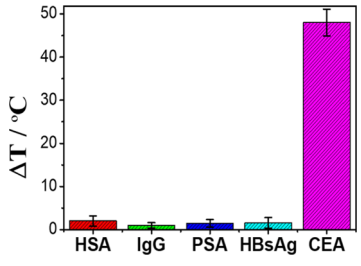

Figure 4. Selectivity of the proposed biosensor for CEA detection. The concentrations of HSA, IgG, PSA, HBsAg, CEA were 1500, 1500, 1500, 1500, and 150 pg/mL, respectively.

has high selectivity in the detection of CEA, which lies in the inherent specificity between the antigen and antibody. Furthermore, the relative standard deviation (SD) was determined to be 4.6% for three measurements (the concentration of CEA was 500 pg/mL), which confirms that the as-proposed biosensor is reproducible for CEA determination.

The long-term stability and the inference of ambient temperature variation were tested to evaluate the stability of the temperature-based immunoassay for CEA detection. As shown in Figure S5, the temperature signal has a negligible change within 20 days, which can attribute to the good airtightness of our designed device. However, temperature variation response was changed after 20 days mainly due to the inference of CO_2 and humidity variation. Therefore, to improve the long-term stability, a suitable airtightness device and dry storage environment are desired. It can be found that this assay is relatively stable at different ambient temperatures (Figure S6). However, the signal response was increased when the ambient temperature was higher than 35 °C. This phenomenon is mostly due to the self-decomposition of H_2O_2 and the increased catalysis ability of PtNPs under a high-temperature environment.

Real Sample Analysis. To investigate the accuracy of the proposed immunosensor for CEA determination in the practical application, we tested 15 serum samples (donated by the volunteers) obtained from the local hospital (Fuzhou, China). The serum samples with unknown CEA concentrations were monitored by the temperature-based testing and compared these results with that obtained from the hospital using chemiluminescence microparticle immunoassay (CMIA), a current "gold standard" strategy of practical detection of CEA in hospitals. As shown in Figure 5A, results of both methods are strongly correlated, showing a linear correlation of $y = 1.021x - 1.582$ (where y denotes the detection value by the CMIA method, and x denotes the detection value by the proposed method) with a correlation coefficient of 0.99. This result reveals that a good consistency is observed between the two methods. In addition, the Bland−Altman plots were constructed to evaluate the agreement between the proposed temperature-based sensing platform and conventional CMIA assay. As shown in Figure 5B, the proposed sensing platform with temperature readout shows a bias offset of −0.5 μg/mL at the limit of agreement (bias ± 1.96 SD) from −18.8 to 17.9 μg/mL for CEA detection compared to the CMIA method. Based on these results, the accuracy of this temperature-based method is nearly the same as that of the conventional CMIA method, indicating the possibility of potential application in the clinical diagnosis.

CONCLUSIONS

In summary, a temperature-based immunosensor using an ordinary thermometer as readout had been established in this study. The designed biosensor successfully transduces the antibody−antigen recognition event into the temperature change with a common thermometer as signal readout. By taking advantages of high catalysis efficiency of nanozyme and self-heating reaction between CaO and H_2O, the quantitative results of CEA can be obtained directly without the assistant of any expensive instruments or power sources other than a simple thermometer. With the merits of high sensitivity, equipment-free, and visual quantitative readout, the as-proposed strategy lays the foundation of thermo-based

DOI: 10.1021/acssensors.9b00968
ACS Sens. 2019, 4, 2375−2380

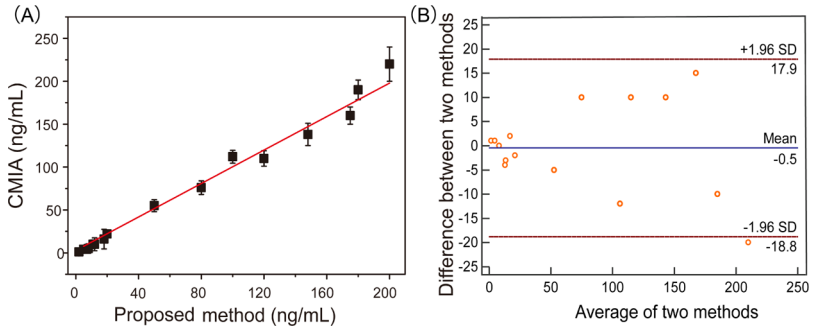

Figure 5. (A) Correlation of the proposed method results with the standard clinical results for CEA detection in 15 serum samples; (B) Bland–Altman analysis for the difference between the proposed method with CMIA for CEA detection in 15 clinical samples.

biosensor applications for diverse targets in the resource-limited area. Besides, materials with higher thermal transformation efficiency or with the naked-eye visualization thermochromism property can be selected as a candidate for further temperature-based biosensor design.

■ ASSOCIATED CONTENT

Supporting Information

The Supporting Information is available free of charge on the ACS Publications website at DOI: 10.1021/acssensors.9b00968.

Materials, apparatus, experimental details, additional images, and tables (PDF)

■ AUTHOR INFORMATION

Corresponding Authors

*E-mail: zylin@fzu.edu.cn (Z.L.).
*E-mail: 18860089899@139.com (G.H.).

ORCID

Xiaoming Ma: 0000-0001-6875-8289
Fang Luo: 0000-0001-7495-450X
Longhua Guo: 0000-0003-0706-0973
Zhenyu Lin: 0000-0001-7890-6812

Notes

The authors declare no competing financial interest.

■ ACKNOWLEDGMENTS

This work was financially supported by NSFC (21804022, 21575025, and 2155027), the Program for Changjiang Scholars and Innovative Research Team in University (no. IRT15R11), the cooperative project of production and study in University of Fujian Province (2018Y4007), the Sciences Foundation of Fujian Province (2018J01685, 2018J01682), STS Key Project of Fujian Province (2017T3007), and the Science and Technology Project of the Education Department of Jiangxi Province of China (no. GJJ170846).

■ REFERENCES

(1) Liu, Y.; Pan, M.; Wang, W.; Jiang, Q.; Wang, F.; Pang, D.-W.; Liu, X. Plasmonic and Photothermal Immunoassay via Enzyme-Triggered Crystal Growth on Gold Nanostars. *Anal. Chem.* **2019**, *91*, 2086−2092.

(2) Jiao, L.; Zhang, L.; Du, W.; Li, H.; Yang, D.; Zhu, C. Au@Pt nanodendrites enhanced multimodal enzyme-linked immunosorbent assay. *Nanoscale* **2019**, *11*, 8798−8802.

(3) Gao, B.; Liu, H.; Gu, Z. An exothermic chip for point-of-care testing using a forehead thermometer as a readout. *Lab Chip* **2016**, *16*, 525−531.

(4) Fu, G.; Sanjay, S. T.; Dou, M.; Li, X. Nanoparticle-mediated photothermal effect enables a new method for quantitative biochemical analysis using a thermometer. *Nanoscale* **2016**, *8*, 5422−5427.

(5) Fu, G.; Sanjay, S. T.; Zhou, W.; Brekken, R. A.; Kirken, R. A.; Li, X. Exploration of Nanoparticle-Mediated Photothermal Effect of TMB-H_2O_2 Colorimetric System and Its Application in a Visual Quantitative Photothermal Immunoassay. *Anal. Chem.* **2018**, *90*, 5930−5937.

(6) Zhang, J.; Xing, H.; Lu, Y. Translating molecular detections into a simple temperature test using a target-responsive smart thermometer. *Chem. Sci.* **2018**, *9*, 3906−3910.

(7) Aytur, T.; Foley, J.; Anwar, M.; Boser, B.; Harris, E.; Beatty, P. R. A novel magnetic bead bioassay platform using a microchip-based sensor for infectious disease diagnosis. *J. Immunol. Methods* **2006**, *314*, 21−29.

(8) Qu, W.; Liu, Y.; Liu, D.; Wang, Z.; Jiang, X. Copper-mediated amplification allows readout of immunoassays by the naked eye. *Angew. Chem., Int. Ed.* **2011**, *50*, 3442−3445.

(9) Wu, L.; Qu, X. Cancer biomarker detection: recent achievements and challenges. *Chem. Soc. Rev.* **2015**, *44*, 2963−2997.

(10) Xiang, Y.; Lu, Y. Using personal glucose meters and functional DNA sensors to quantify a variety of analytical targets. *Nat. Chem.* **2011**, *3*, 697−703.

(11) Song, Y.; Wang, Y.; Qin, L. A Multistage Volumetric Bar Chart Chip for Visualized Quantification of DNA. *J. Am. Chem. Soc.* **2013**, *135*, 16785−16788.

(12) Ma, X.; Chen, Z.; Zhou, J.; Weng, W.; Zheng, O.; Lin, Z.; Guo, L.; Qiu, B.; Chen, G. Aptamer-based portable biosensor for platelet-derived growth factor-BB (PDGF-BB) with personal glucose meter readout. *Biosens. Bioelectron.* **2014**, *55*, 412−416.

(13) Song, Y.; Xia, X.; Wu, X.; Wang, P.; Qin, L. Integration of Platinum Nanoparticles with a Volumetric Bar-Chart Chip for Biomarker Assays. *Angew. Chem., Int. Ed.* **2014**, *53*, 12451−12455.

(14) Pappas, L.; Foglierini, M.; Piccoli, L.; Kallewaard, N. L.; Turrini, F.; Silacci, C.; Fernandez-Rodriguez, B.; Agatic, G.; Giacchetto-Sasselli, I.; Pellicciotta, G.; Sallusto, F.; Zhu, Q.; Vicenzi, E.; Corti, D.; Lanzavecchia, A. Rapid development of broadly influenza neutralizing antibodies through redundant mutations. *Nature* **2014**, *516*, 418−422.

(15) Gu, C.; Lan, T.; Shi, H.; Lu, Y. Portable Detection of Melamine in Milk Using a Personal Glucose Meter Based on an in Vitro Selected Structure-Switching Aptamer. *Anal. Chem.* **2015**, *87*, 7676−7682.

(16) Zhao, M.; Wang, P.; Guo, Y.; Wang, L.; Luo, F.; Qiu, B.; Guo, L.; Su, X.; Lin, Z.; Chen, G. Detection of aflatoxin B_1 in food samples based on target-responsive aptamer-cross-linked hydrogel using a handheld pH meter as readout. *Talanta* **2018**, *176*, 34−39.

(17) Wang, A.; Ma, X.; Ye, Y.; Luo, F.; Guo, L.; Qiu, B.; Lin, Z.; Chen, G. A Simple and Convenient Aptasensor for Protein Using an Electronic Balance as a Readout. *Anal. Chem.* **2017**, *90*, 1087−1091.

DOI: 10.1021/acssensors.9b00968
ACS Sens. 2019, 4, 2375−2380

(18) Mahalik, N. P.; Nambiar, A. N. Trends in food packaging and manufacturing systems and technology. *Trends Food Sci. Technol.* **2010**, *21*, 117−128.
(19) Lee, S.; Kwon, D.; Yim, C.; Jeon, S. Facile detection of Troponin I using dendritic platinum nanoparticles and capillary tube indicators. *Anal. Chem.* **2015**, *87*, 5004−5008.
(20) Gao, Z.; Xu, M.; Hou, L.; Chen, G.; Tang, D. Irregular-shaped platinum nanoparticles as peroxidase mimics for highly efficient colorimetric immunoassay. *Anal. Chim. Acta* **2013**, *776*, 79−86.
(21) Zhu, Z.; Guan, Z.; Liu, D.; Jia, S.; Li, J.; Lei, Z.; Lin, S.; Ji, T.; Tian, Z.; Yang, C. J. Translating Molecular Recognition into a Pressure Signal to enable Rapid, Sensitive, and Portable Biomedical Analysis. *Angew. Chem., Int. Ed.* **2015**, *54*, 10448−10453.
(22) Bai, X.-R.; Wang, L.-H.; Ren, J.-Q.; Bai, X.-W.; Zeng, L.-W.; Shen, A.-G.; Hu, J.-M. Accurate Clinical Diagnosis of Liver Cancer Based on Simultaneous Detection of Ternary Specific Antigens by Magnetic Induced Mixing Surface-Enhanced Raman Scattering Emissions. *Anal. Chem.* **2019**, *91*, 2955−2963.
(23) Liu, H.; Rong, P.; Jia, H.; Yang, J.; Dong, B.; Dong, Q.; Yang, C.; Hu, P.; Wang, W.; Liu, H.; Liu, D. A wash-free homogeneous colorimetric immunoassay method. *Theranostics* **2016**, *6*, 54.
(24) Zhang, X.; Ding, S.-N. General Strategy to Fabricate Electrochemiluminescence Sandwich Type Nanoimmunosensors Using CdTe@ZnS Quantum Dots as Luminescent Labels and Fe3O4@SiO2' Nanoparticles as Magnetic Separable Scaffolds. *ACS Sens.* **2016**, *1*, 358−365.
(25) Li, H.; Shi, L.; Sun, D.-e.; Li, P.; Liu, Z. Fluorescence resonance energy transfer biosensor between upconverting nanoparticles and palladium nanoparticles for ultrasensitive CEA detection. *Biosens. Bioelectron.* **2016**, *86*, 791−798.
(26) Miao, H.; Wang, L.; Zhuo, Y.; Zhou, Z.; Yang, X. Label-free fluorimetric detection of CEA using carbon dots derived from tomato juice. *Biosens. Bioelectron.* **2016**, *86*, 83−89.
(27) He, M.-Q.; Wang, K.; Wang, W.-J.; Yu, Y.-L.; Wang, J.-H. Smart DNA Machine for Carcinoembryonic Antigen Detection by Exonuclease III-Assisted Target Recycling and DNA Walker Cascade Amplification. *Anal. Chem.* **2017**, *89*, 9292−9298.
(28) Fu, Q.; Wu, Z.; Du, D.; Zhu, C.; Lin, Y.; Tang, Y. Versatile Barometer Biosensor Based on Au@Pt Core/Shell Nanoparticle Probe. *ACS Sens.* **2017**, *2*, 789−795.

DOI: 10.1021/acssensors.9b00968
ACS Sens. 2019, 4, 2375−2380